Dandao Xuebao/Journal of Ballistics
ISSN: 1004-499X
Vol. 36 No. 1 (2024)

Phase, Minero-Chemical and Microstructural Characterization of Chromite Ore

Sajjad Ali[1], Salar Ahmad[2*], Asghar Ali[3], Amir Shahzad[4], Muhammad Naeem Tabassum[5], Muhammad Zahid Khan[6], Farman Ullah[2], Javaid Khan[7]

[1]Materials Research Laboratory, Department of Physics, University of Peshawar, 25120 Pakistan

[2]Department of Physics, Government Post Graduate College Timergara, Lower Dir, 18300, Pakistan

[3]Department of Geology, University of Peshawar, Peshawar, 25120, Pakistan

[4]College of Electronics and Information Engineering, Shenzhen University, Shenzhen, 518060, China

[5]College of Physics and Optoelectronics engineering, Shenzhen University, Shenzhen, 518060, China

[6]Department of Physics, Gomal University Dera Ismail Khan, 29111, KPK, Pakistan

[7]Department of applied Physics, Nanjing University of Science and Technology, Nanjing, 210094, China

*ahmadsalar430@gmail.com

ABSTRACT

Chromite ore sample was collected from active mine of Heroshah (34.503041 °N, 71.904565 °E) Malakand agency, Khyber Pakhtunkhwa (KP), Pakistan. The sample was properly washed, dried, and grounded to 74 μm (200 mesh) in a pestle and mortar. The phase, microstructure and chemical composition of the ore was studied. X-rays diffraction (XRD) analysis revealed the presence of Aluminium chromite [$Fe(Al,Cr)_2O_4$] and Ringwoodite (Mg_2SiO_4) phases. Microstructural study revealed granular morphology where the chromite grains were surrounded by veins and grains of gangue material. It also shows fractures filled with gangue minerals. Elemental analysis confirmed the presence of high content of Chromium (43% on average) and iron (18% on average) in the as mined sample along with some proportion of Mg, Al and Si. Moreover, Fourier transform infra-red (FTIR) spectroscopy revealed the characteristic bands of chromium oxides (Cr^{+2}-O^{-2}).

Key words: Chromite ore; Microstructure; Grains; X-ray diffraction; Phase

1. Introduction

Chromite ore is widely used as a raw material for the production of sodium dichromate and different other chromium compounds [1]. Throughout the 20th Century, chromite ore has been used in pigments for textiles and paint, strengthening leather processing and timber maintenance, synthesizing catalysts for chemicals, preserving surface treatments and protecting stainless steel and non-ferrous alloys [2, 3]. According to estimates, the metallurgy, chemical, and refractory industries in USA uses 87%, 10%, and 3% of the country's chromium respectively [4].

Chaudhry et al. [5] studied the phase composition of chromite ore and found cobalt Chromite as the major phase along with the Average crystallite size and micro-strain (17.91 nm) and ($-$ 9.86 × 10−4) respectively. They noticed a large surface to volume ratio for the collected samples. Chromite ore having grainular morphology with varying particle size has been reported by Das et al. [6] along with textures and cracks which are filled with secondary minerals. These minerals are formed during weathering cycles and its main constituents are gibbsite, kaolinite, hematite, and goethite [6]. Chrysochoou et al. [7] also reported textural morphology with cracks and found that it is actually the minerology which determine the reaction pathway model. For the accurate determination of Chromium content in the obtained Chromium ore residue from two sites, Matern et, al. [8] evaluated two digestion methods. Moreover, Dermatas et al. [9] found a large amount of Silica content in the Chromite ore residue.

The present study cannot be only associated to the site in Malakand Pakistan because in USA [9-11] and Europe [12-14] the minerology and characterization of Chromite ore have already been evaluated and it has been found that the Chromite ore samples possess different mineralogical compositions. Differences in extraction process, deposition techniques and ambient weathering conditions are responsible for the different compositions of the Chromite ore [8].

Due to the increase in population and government emphasis on industrialization in Pakistan, the demand for ferro alloys is increasing day by day. This directly made it inevitable to investigate the locally available resources of ferro alloys as well as Chromite ore. The present study investigates the chemical, mineralogical and microstructural characteristics of chromite ore obtained from the Northern Indus Suture Zone Dargai, Pakistan. Because of the short time of land falling, the leaching time is limited, we expect a high chromium content in these samples. The results presented in this study provides understanding of the obtained samples and are essential for extraction of Cr from this ore in future.

2. Regional Geology of Malakand Chromite ore

Primary metallic ore minerals are often linked with the ultramafic, mafic, and felsic igneous rocks that form as a result of fractional crystallization of a homogeneous magma [15]. Fractional crystallization of magma causes segregates into economically viable deposits in different types of igneous rocks. It is widely discerned that spinel group, chalcophile/siderophile and lithophile are respectively associated with mafic ultramafic, and felsic igneous rocks. Ultramafic igneous rocks that comprise the lower ocean crust and upper mantle emplaced onto a continental crust in collisional orogenic belts by obduction processes [16]. These rocks contain podiform chromite deposits derived from the fractionation of mid oceanic ridge basalt [17]. Ophiolite hosting chromite deposits are commonly exposed along the convergent plate margin due to obduction of the remnant intervening oceanic crust onto a continental crust [18]. Ophiolite hosting chromite deposits occur in lenses with a mixture of olivine that crystallize from mid oceanic ridge basalt at ~1200°C, the olivine later alter to serpentine due to metasomatism [19].

Chromite deposits are mined in Europe, Asia, Africa, North and South America and Australia. The Neotethyan ophiolites are nicely exposed along the nearly E−W trending Alpine-Himalayan Orogenic belt [20]. Pakistan has been well-known for its chromite bearing Neotethyan ophiolites exposed at the northern Indus suture zone termed Main Mantle Thrust in Pakistan and western Kurram−Waziristan−Zhob−Muslim Bagh−Bela Ophiolite Belt [20]. The ultramafic portion of the Dargai Ophiolitic complex comprises dunite, wehrlite, harzburgite, chromitite, pyroxenite dikes and serpentinite [21]. The Dargai ophiolitic complex has subdivided into an intra-oceanic subduction and MOR associated ophiolites through micro analyzer (electron probe) and plasma mass spectrometer (inductively-coupled) mineral chemistry [21]. The intra oceanic subduction ophiolite contains high concentration of chromium, whereas the MOR affinity ophiolite comprises high aluminum. These different geochemical characteristics indicate that the Dargai chromitite parental magma evolved from the mid oceanic ridge basalt and supra-subduction zone [21]. Further detail of Dargai Ophiolitic complex is shown in Figure 1.

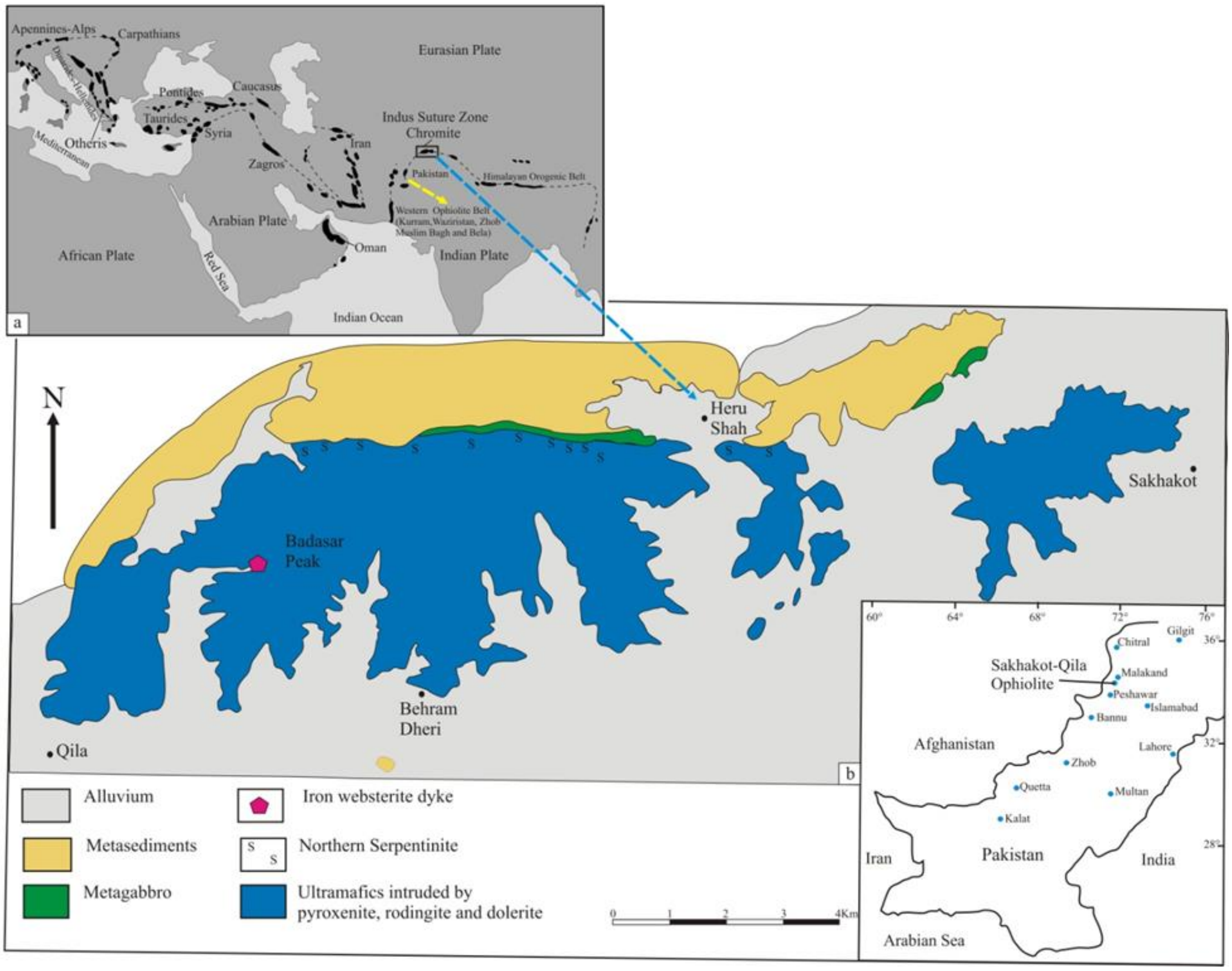

Figure 1: (a) Regional geological map of the Alpine−Himalayan Orogenic belt showing E−W distribution of the Tethyan ophiolites. (b) Local geological map of the study area indicating the northern Indus Suture Zone Dargai ophiolite Complex exposed in a E−W trending tectonically klippe onto the Indian plate metasediments [22].

3. Materials and methods

Chromite ore samples were taken from an operational mine in Heroshah, Malakand Agency, Khyber Pakhtunkhwa (KP), Pakistan (34.503041 °N, 71.904565 °E). The deionized water-washed samples were thoroughly dried in a hot-air oven (FREAS 605, Thermo Fisher Scientific, USA) overnight at 90°C before being crushed and ground in a stainless-steel pestle and mortar arrangement. Using a PMG-3 microscope and a DP-12CCD camera (Olympus, Japan), the samples' reflected light optical microscopic images were captured. Utilizing X'Pert3 Powder (PANalytical, Netherlands) XRD, the sample's crystalline phases were identified. CuKα radiations (λ=1.54Å), at an operational voltage of 40 kV, current of 30 mA, a count rate of 1.0 s/step, and a step size of 0.03°, were used to scan the sample from 2θ=10° to 70°. A SEM (JEOL JSM 5910) fitted with an INCA200, Oxford Instruments, UK EDS detector was used for the morphological microstructural studies and elemental studies. To achieve this, pieces measuring ~4×4×4 were cut using a TeckCut 4^{TM} precision low speed diamond saw (Allied High Tech. Products, USA). Using a TwinPrep 3^{TM} grinding and polishing machine, the samples were polished to a fine luster while being lubricated with water. Imperial sticky back polishing cloths with several grades of silicon carbide paper and diamond paste were used. The polished, flat surfaces were etched chemically for one minute in hydrofluoric acid (40%) fumes. In order to prevent charging in the SEM, Silver paint and gold coating was used, and the polished sample was mounted onto Aluminium stubs.

4. Results & discussion

4.1 X-ray Analysis

The room temperature XRD pattern recorded for as-mined chromite ore is shown in Figure 2. The relative intensities for the primary XRD peaks (designated as *) observed for this sample matched PDF # 1-1129 for Aluminium Chromite [Fe (Al, Cr)$_2$O$_4$], indicating that it is the dominant phase in the sample under investigation. Moreover, a few minor peaks (labelled as +) matched PDF # 13-230 showing Ringwoodite (Mg_2SiO_4) phase. The peak with maximum intensity indicates that the sample possess textures and must contain grains. A major $FeAl_2O_4$ phase in addition with small amounts of SiO_2 in chromite ore was also reported by Zhang, et al [23]. Another XRD study by Chen, et al [24] noticed Cr_2O_3 as major phase together with trace amounts of FeO, MgO, Al_2O_3, SiO_2 and MnO in chromite ore.

The average crystallite size D (nm), the average micro strain (ε) and dislocation density were computed by using equations (1) (Scherrer formula) [25], equation (2) [26] and equation (3) [27] respectively. The average particle size and micro strain of the sample were computed to be 26.25 nm and 578.42 respectively as shown in table 1. The small value of crystallite size accounts for high ordering within the Obtained Chromite ore samples which arises due to breaking of bonds. Consequently, the crystallite size decreases due to this bond breaking [28]. Table 2 show that that sample's micro strain is inversely proportional to its particle size. The high value of micro strain depicts that the sample possess microstructural textures and fractures which are further confirmed by the reflected light micrograph and SEM analysis [29].

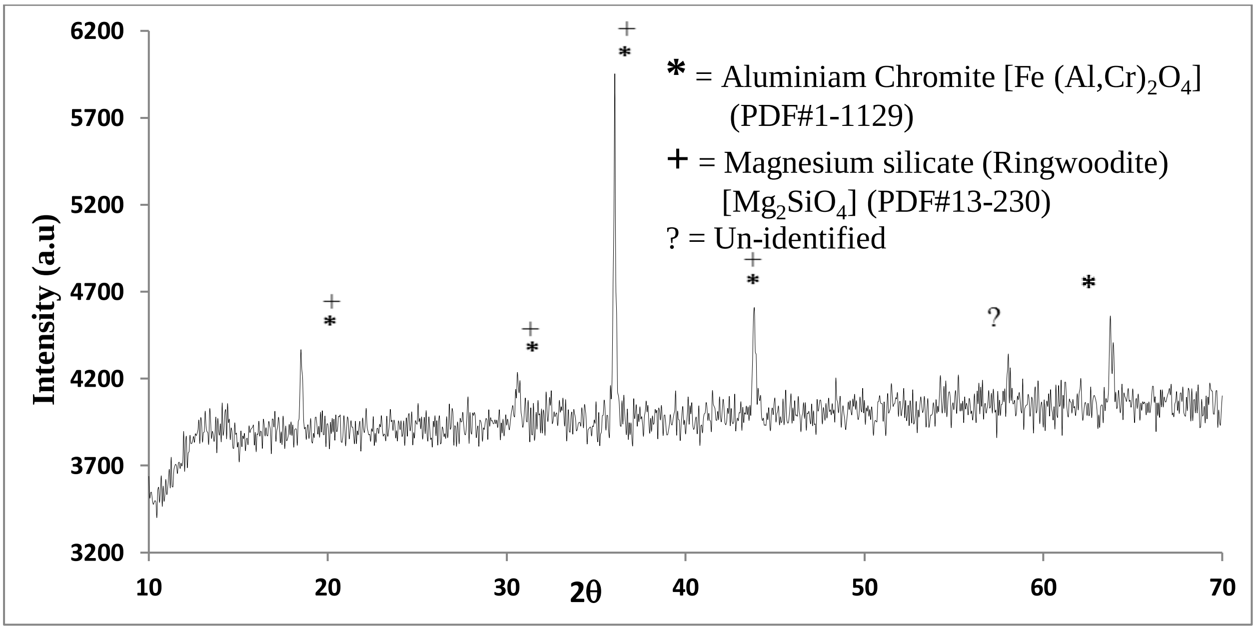

Figure 2: XRD pattern of as-mined chromite ore indicating the presence of major and minor phases marked as * and + respectively.

Table 1: The average crystallite size, micro strain, and dislocation density of chemically etched as mined chromite ore.

Peak position (2theta)	FWHM	Crystallite size D (nm)	ε * 10^-3	Average D(nm)	δ * 10^-3 (nm^-2)	Average ε
0.14544	0.17124	46.392	588.69	26.25	1.451	578.51
28.46895	33.51962	0.244	576.54			
0.15271	0.1798	44.18	588.69			
0.18108	0.2132	37.26	588.68			
56.7523	66.82072	0.135	539.76			
0.2304	0.27128	29.28	588.71			

$$D = 0.89\lambda / \beta \cos\theta \tag{1}$$

Where, D represents the average crystallite size, wavelength of X-rays is designated as λ, FWHM is represented as β and θ is angle of diffraction.

$$\varepsilon = \beta/4 \tan\theta \tag{2}$$

Here, ε represents micro strain, β is the FWHM and θ is the diffraction angle.

$$\delta=1/D^2 \tag{3}$$

Here, δ gives the dislocation density while D represents the average crystallite size.

4.2 Reflected light microscopic analysis

In geological terms, chromite ores are called orthogenetic ores i.e., formed by ‘magnetic segregation’, meaning that chromite crystals either settle together at early stage when the magma is in molten state, or they are accumulated by gravitational pull in the liquid form of magma. This statement is very much important in understanding the layered structure of chromite ore as the ore is always present in the form of layered masses, lenses or diffused in the host rocks [30, 31]. The presence of distinct micro-regions with irregular shapes which possess separations by sharp boundaries are shown in figure 3 by the reflected light micrograph of etched (40% HF fumes for 50 sec) chromite ore. X-ray analysis also reported that the sample contain textures and grains hence our results are in line.

Reflected light microscopic study of chromite sample suggested that the surface color varies from pale grey to brown, grey and greenish grey as shown in Figure 3. The individual grains are coarse with distinct boundaries. In most cases, the grain boundaries appear corroded. There are fractures in the grains which are replaced by ringwoodite and later on converted into grain boundaries. Compounds of ringwoodite are Mg rich which are usually colorless to pale yellow to golden yellow while the relatively dark colors correspond to higher silica contents. Grains display a distinctive irregular fracture patterns which are recognized by their high birefringence, distinctive fracturing, and lack of cleavage.

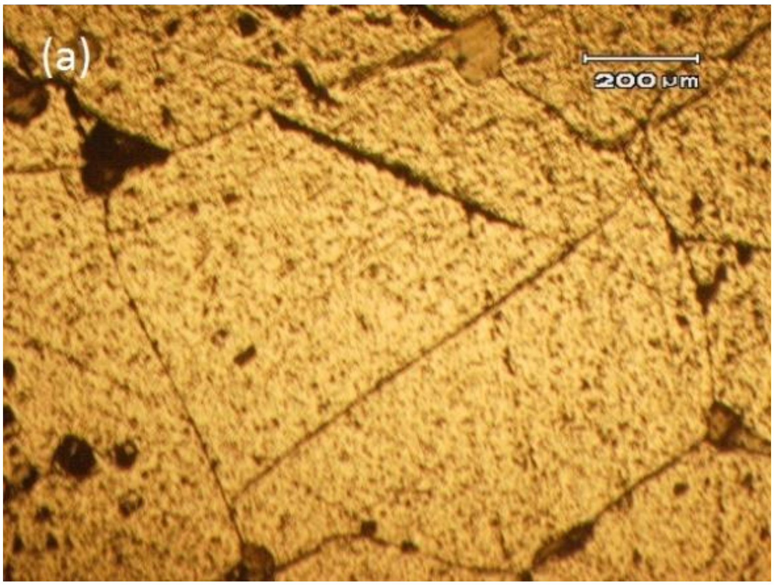

Figure 3: Reflected light micrograph of chemically etched as-mined chromite ore.

4.3 Scanning electron microscopic (SEM) and EDS analysis

Figure 4 shows scanning electron microscope SEM image of as-mined chromite ore. The micro-regions marked as “A” and “C” were chromite rich as given in Table 2 with relatively higher chromite concentrations. These micro-regions were irregular in shape separated by sharp and distinct boundaries. X-ray analysis confirmed that the sample contain grains which are confirmed by the SEM micrograph of figure 4. The elemental and oxide compositions of different micro-regions derived from EDS data are listed in table 2 which confirmed the presence of chromite and ringwoodite in the investigated sample. Ringwoodite is a commonly occurring impurity in chromite but the high silica content makes the relevant chromite unsuitable for use in metallurgical industry in arc furnaces [32]. From figure 4, chromite phases reflects a greenish grey color whereas the ringwoodite micro-regions are relatively darker in color. The chromium content decreases with increasing silicon content. Ahmad et al., also found that the nano-particles are embedded in silicate layer [25].

Figure 4 show that the grains are of different structures which indicates the different degrees of crystallization of different mineral phases present in Chromite ore. It also reflects the diverse concentration of the elements which are reported in table 2. Bonifazi et al. [33] also found that the morphology of chromite ore is rarely isomorphic. They attributed the different morphology of the grains to the remobilization of Cr, Al and Mg ions which causes serpentinization. Weight percents of the corresponding oxides are also reported by table 2.

The textural behaviour which was previously reported by X-ray analysis is further confirmed by figure 4. We can notice from figure 4 that the fractures are filled which is due to the redeposition of gangue minerals. Similar redepositions of gangue minerals was reported by Bonifazi et al [33]. Figure 5 (a, b, c and d) shows the elemental composition (by weight percent) of region A, B, C and D respectively.

Table 2: The average EDS-derived elemental and oxide compositions of the micro-regions labeled as A, B, C and D in figure 4.

Phases	**EDS Data**		**Oxide Form**	
	Element	wt.%	Oxide	wt. %
A	Mg	16.11	MgO	17.18
	Al	22.25	Al_2O_3	26.99
	Cr	43.49	Cr_2O_3	40.82
	Fe	18.15	Fe_2O_3	16.39
B	Mg	46.71	MgO	42.19
	Si	44.25	SiO_2	51.48
	Fe	9.04	Fe_2O_3	16.39
C	Mg	15.05	MgO	16.01
	Al	23.07	Al_2O_3	27.93
	Cr	44.86	Cr_2O_3	42.01
	Fe	17.03	Fe_2O_3	16.39
D	Mg	19.86	MgO	18.23
	Si	48.38	SiO_2	57.22
	Ca	27.64	CaO	21.38
	Cr	2.42	Cr_2O_3	1.95
	Fe	1.69	Fe_2O_3	16.39

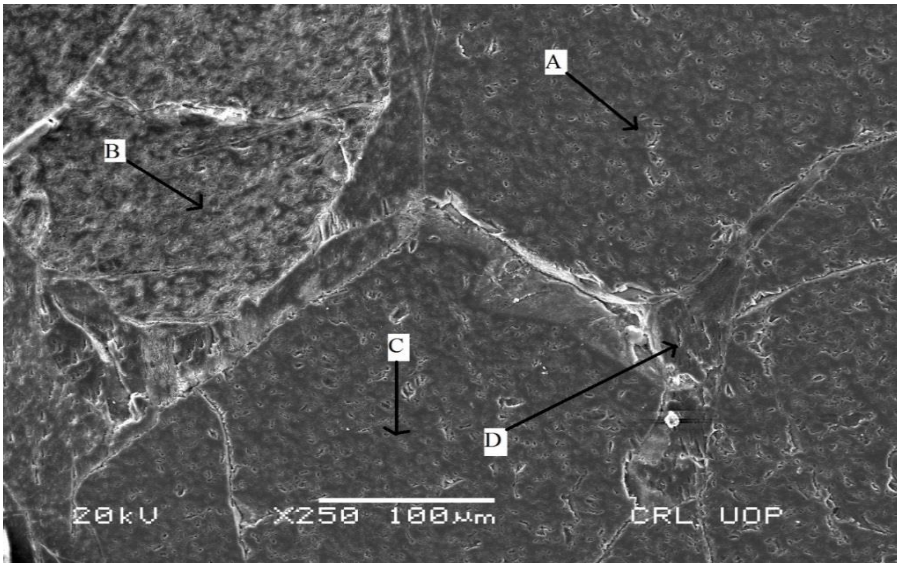

Figure 4: SEM of as-mined chromite ore with different micro-regions labeled as A, B, C and D.

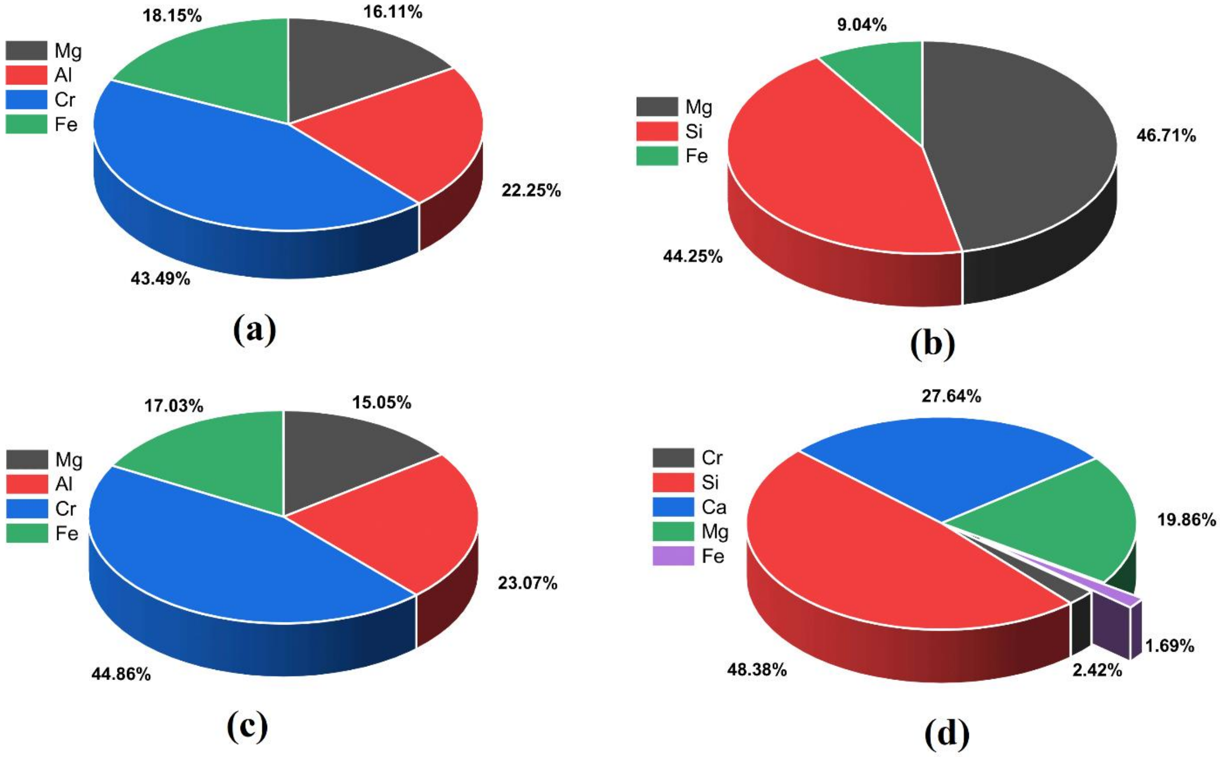

Figure 5: (a), (b), (c) and (d) representing the weight percents of elements for the selected regions A, B, C and D in fig 4 respectively.

4.4 (FTIR) analysis

Figure 6 shows the FTIR spectra of chromite ore carried out in the range 400 –4000 cm^{-1}. Due to M-O and Cr-O stretching frequencies, the transition metal chromite spinals are anticipated to exhibit the characteristic absorption bands in the short wavelength region between 690-650 cm^{-1} [34]. The band at 653 cm^{-1} confirm the spinel chromite which appears because of the stretching vibrations of Cr^{+2}-O^{-2} [5]. The Co(II)-O bond is confirmed by the band at 886 cm^{-1} [5].

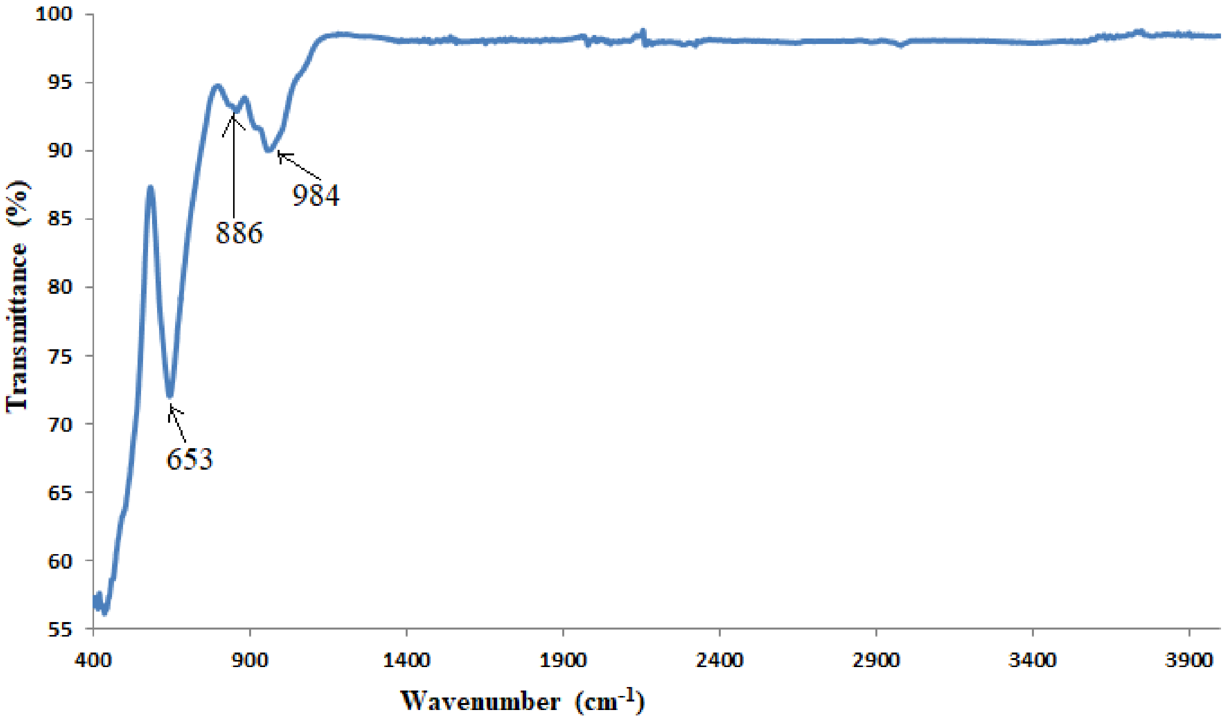

Figure 6: FTIR spectra of the chemically etched as mined Chromite ore.

5. Conclusion

Minero-chemical, phase and microstructural study of Chromite ore collected from Heroshah, Malakand agency, Pakistan has been successfully presented. X-ray analysis confirmed Al-Chromite as a major phase. The higher Average micro strain (ε) show the hardness and tough nature of the obtained samples. EDS analysis reports high content of Chromium which is the most important constituent of Chromite ore and can be utilized in inducing hardness, toughness, and chemical resistance in steel. SEM analysis confirmed that the obtained sample possess filled-fractures which accounts for a high percentage of mixed minerals within the obtained chromite ore. These filled fractures enhance the strength and reflects its use in different industries. Moreover, all our results are in line with each other.

Data availability

No data has been generated for this research. All the experiments performed and their results are presented in the paper.

Author Contributions

Sajjad Ali performed the experimental work, Salar Ahmad contributed in writing the paper and exploring the experimental results, Asghar Ali performed the regional geology, Amir Shahzad contributed in making the tables, Muhammad Naeem Tabassum helped in calculations, Muhammad Zahid Iqbal helped in exploring the results, Farman Ullah and Javaid Khan contributed in review.

Competing interests

The authors declare no competing interests.

References

1. Baba, A.A., et al., *Preparation of Industrial Sodium Chromate Compound from an Indigenous Chromite Ore by Oxidative Decomposition*, in *Rare Metal Technology 2021*. 2021, Springer. p. 239-245.
2. Firth, I. and R. Capil, *Metals in the workplace*, in *Principles of Occupational Health & Hygiene*. 2020, Routledge. p. 207-241.
3. Ostadrahimi, M., et al., *Effect of iron bearing minerals on iron ore processing.* 2024: p. 25726641241265201.
4. Rahman, Z., V.P.J.E.m. Singh, and assessment, *The relative impact of toxic heavy metals (THMs)(arsenic (As), cadmium (Cd), chromium (Cr)(VI), mercury (Hg), and lead (Pb)) on the total environment: an overview.* 2019. **191**(7): p. 1-21.
5. Choudhary, P., et al., *Weak ferroelectricity and leakage current behavior of multiferroic CoCr2O4 nanomaterials.* 2019. **32**(8): p. 2639-2645.
6. Das, S.J.I.J.o.M., Metallurgy, and Materials, *Quantitative mineralogical characterization of chrome ore beneficiation plant tailing and its beneficiated products.* 2015. **22**: p. 335-345.
7. Chrysochoou, M., et al., *Importance of mineralogy in the geoenvironmental characterization and treatment of chromite ore processing residue.* 2010. **136**(3): p. 510-521.
8. Matern, K., H. Kletti, and T.J.C. Mansfeldt, *Chemical and mineralogical characterization of chromite ore processing residue from two recent Indian disposal sites.* 2016. **155**: p. 188-195.
9. Dermatas, D., et al., *Chromite ore processing residue (COPR): Hazardous contaminated soil or solid waste?* 2006. **1482**: p. 145.
10. Boecher, T., et al., *Quantification of mineralogical and amorphous species in chromium ore processing residue.* 2012. **9**(4): p. 131-141.
11. Chrysochoou, M. and D.J.J.o.h.m. Dermatas, *Application of the Rietveld method to assess chromium (VI) speciation in chromite ore processing residue.* 2007. **141**(2): p. 370-377.
12. Geelhoed, J.S., et al., *Identification and geochemical modeling of processes controlling leaching of Cr (VI) and other major elements from chromite ore processing residue.* 2002. **66**(22): p. 3927-3942.
13. Hillier, S., et al., *Role of quantitative mineralogical analysis in the investigation of sites contaminated by chromite ore processing residue.* 2003. **308**(1-3): p. 195-210.
14. Thomas, R., et al., *Analytical characterisation of solid-and solution-phase chromium species at COPR-contaminated sites.* 2001. **23**: p. 195-199.
15. Smith, J.M., et al., *Magmatic origin for the massive sulfide ores in the sedimentary country rocks of mafic–ultramafic intrusions in the Midcontinent Rift System.* 2022: p. 1-22.
16. Ali, A., et al., *Tectonic Framework of Northern Pakistan from Himalaya to Karakoram*, in *Structural Geology and Tectonics Field Guidebook—Volume 1*. 2021, Springer. p. 367-412.
17. Zhou, M.-F., et al., *Compositions of chromite, associated minerals, and parental magmas of podiform chromite deposits: The role of slab contamination of asthenospheric melts in suprasubduction zone environments.* 2014. **26**(1): p. 262-283.
18. Pirajno, F., I. Uysal, and E.A.J.G.R. Naumov, *Oceanic lithosphere and ophiolites: Birth, life and final resting place of related ore deposits.* 2020. **88**: p. 333-352.
19. Aïfa, T.J.G.S., London, Special Publications, *Mineralization and sustainable development in the West African Craton: from field observations to modelling*. 2021, Geological Society of London. p. 1-29.
20. Cvetkovic, V., D. Prelević, and S. Schmid, *Geology of south-eastern Europe*, in *Mineral and thermal waters of Southeastern Europe*. 2016, Springer. p. 1-29.
21. Ullah, Z., et al., *Petrochemistry of high-Cr and high-Al chromitites occurrences of dargai complex along indus suture zone, northern Pakistan.* 2020. **43**(2): p. 689-709.

22. Ahmed, Z.J.C.g., *Comparison of the geochemistry of ophiolitic pyroxenites with a strongly fractionated dyke of pyroxenite from the Sakhakot-Qila Ophiolite, Pakistan.* 1991. **91**(4): p. 335-355.
23. Zhang, H., et al., *Pressure oxidative leaching of Indian chromite ore in concentrated NaOH solution.* 2014. **142**: p. 47-55.
24. Chen, G., et al., *A new metallurgical process for the clean utilization of chromite ore.* 2014. **131**: p. 58-68.
25. Ahmad, S., et al., *Synthesis and characterization of manganese ferrite from low grade manganese ore through solid state reaction route.* 2021. **11**(1): p. 1-9.
26. Shirsath, S.E., et al., *Structural and magnetic properties of In3+ substituted NiFe2O4.* 2009. **117**(1): p. 163-168.
27. Rao, S.D.S., et al., *Structural Optical properties of Zinc Oxide (ZnO) Nano Particles.*
28. Rathi, A., et al., *Anomalous nano-magnetic effects in non-collinear spinel chromite NiCr2O4.* 2019. **474**: p. 585-590.
29. Nadammal, N., et al., *Critical role of scan strategies on the development of microstructure, texture, and residual stresses during laser powder bed fusion additive manufacturing.* 2021. **38**: p. 101792.
30. Duke, J.J.G.C., *Ore deposit models 7. Magmatic segregation deposits of chromite.* 1983. **10**(1): p. 15-24.
31. Mirza, T.A.J.U.P.T.U.o.S., 189p, *Petrogenesis of the Mawat ophiolite complex and the associated chromitite, Kurdistan Region, NE Iraq.* 2008.
32. Wills, B.A. and J. Finch, *Wills' mineral processing technology: an introduction to the practical aspects of ore treatment and mineral recovery*. 2015: Butterworth-Heinemann.
33. Bonifazi, G. and S.J.S.m. Mati, *Characterization of Kalimashi chromite ore (Albania) by scanning electron microscopy.* 1990. **4**(2): p. 3.
34. Pirogova, G., et al., *Catalytic properties of spinel-type complex oxides in oxidation reactions.* 1994. **43**(10): p. 1634-1636.